

## Proton inelastic scattering in $^{68,70,72}\text{Ni}$ isotopes

L. SCOMPARIN<sup>(1)(2)(\*)</sup>, T. MARCHI<sup>(2)(\*\*)</sup>, G. DE ANGELIS<sup>(2)</sup>, T. BAUMANN<sup>(4)</sup>,  
D. BAZIN<sup>(4)</sup>, A. GADE<sup>(4)</sup>, A. GOTTARDO<sup>(2)</sup>, F. GRAMEGNA<sup>(2)</sup>, P. R. JOHN<sup>(9)(1)(3)</sup>,  
M. KLINTEFJORA<sup>(8)</sup>, K. KOLOS<sup>(11)</sup>, S. M. LENZI<sup>(1)(3)</sup>, D. MENGONI<sup>(1)(3)</sup>,  
C. MICHELAGNOLI<sup>(7)</sup>, V. MODAMIO<sup>(8)</sup>, D. R. NAPOLI<sup>(2)</sup>, S. NOJI<sup>(4)</sup>, J. PEREIRA<sup>(4)</sup>,  
F. RECCHIA<sup>(4)</sup>, E. SAHIN<sup>(8)</sup>, J. J. VALIENTE-DOBÓN<sup>(2)</sup>, K. WIMMER<sup>(10)</sup>,  
D. WEISSHAAR<sup>(4)</sup> and R. ZEGERS<sup>(4)(5)(6)</sup>

<sup>(1)</sup> *Department of Physics and Astronomy, University of Padua - Padua, Italy*

<sup>(2)</sup> *INFN, Legnaro National Laboratories - Legnaro, Italy*

<sup>(3)</sup> *INFN, Section of Padua - Padua, Italy*

<sup>(4)</sup> *NSCL, Michigan State University - East Lansing (MI) 48824, USA*

<sup>(5)</sup> *Joint Inst. for Nuclear Astrophysics, Michigan State University - East Lansing (MI), USA*

<sup>(6)</sup> *Dept. of Physics and Astronomy, Michigan State University - East Lansing (MI), USA*

<sup>(7)</sup> *Institut Laue-Langevin (ILL) - 38042 Grenoble Cedex 9, France*

<sup>(8)</sup> *Department of Physics, University of Oslo - Blindern, N-0316 Oslo, Norway*

<sup>(9)</sup> *Institut für Kernphysik, Technische Universität Darmstadt - Darmstadt, Germany*

<sup>(10)</sup> *Instituto de Estructura de la Materia, CSIC - E-28006 Madrid, Spain*

<sup>(11)</sup> *Lawrence Livermore National Laboratory - Livermore, CA 94551, USA*

received 15 January 2021

**Summary.** — A preliminary analysis of the proton inelastic scattering of  $^{68,70,72}\text{Ni}$  at intermediate energies will be discussed. This measurement is important for the study of the nuclear shell's evolution in the nickel isotopic chain. A brief description of the physics case, the setup, and the particle identification methods will be presented.

### 1. – Introduction

The evolution of nuclear shells along isotopic and isotonic chains is a well established fact in today's nuclear physics. The nuclear force, indeed, hides complex features that appear in particular regions of the nuclear chart when unbalanced neutron to proton ratio conditions are reached. The observation of neutron halos in light systems, the inversion

(\*) E-mail: [luca.scomparin@lnl.infn.it](mailto:luca.scomparin@lnl.infn.it)

(\*\*) E-mail: [tommaso.marchi@lnl.infn.it](mailto:tommaso.marchi@lnl.infn.it)

of nuclear shells or the appearance of new magic numbers are stunning examples of the peculiar behavior of the nuclear system that require a careful revision of the classical formulation of the well established Nuclear Shell model. A comprehensive summary on the present knowledge of both theoretical and experimental manifestations of Shell Evolution is given by Otsuka and collaborators in a recent review [1].

In this work the evolution of collectivity along the nickel isotopic chain ( $Z = 28$ ) will be considered, with particular interest on the neutron-rich side towards the doubly magic  $^{78}\text{Ni}$ . At the experimental level, basic information about collectivity in even-even isotopes is usually obtained from two observables: the energy of the first ( $2^+$ ) excited state and the related transition probability towards the ground state. In the latter case, the reference quantity is usually the reduced transition probability  $B(E2; 0^+ \rightarrow 2^+)$ , namely the normalized electromagnetic transition amplitude [2]. This quantity is also inversely proportional to the lifetime of the nuclear state. Excitation energies can be measured directly and with high resolution. Likewise, transition probabilities can be directly extracted from lifetime measurements. On the other hand, indirect measurements can be performed by using excitation cross sections. In this case, two main reaction mechanisms are commonly used: Coulomb Excitation (Coulex) and proton inelastic scattering. Coulex or lifetime measurements can be considered electromagnetic probes in the case of a safe impact parameter selection (Safe Coulex) and of vanishing non-electromagnetic decay, respectively. Under these conditions they are sensitive only to proton contributions. Proton scattering, on the contrary, is affected by both protons and neutrons. This difference provides an important tool for understanding the relative weight of valence and core components of the transitions. Several measurements have been performed along the nickel isotopic chain and are reported in the literature [3-9].

Moving one step forward, the nuclear degree of collectivity can also be seen in terms of the quadrupole deformation parameter  $\beta_2$  that can be extracted from electromagnetic transition amplitudes, or from the deformation length evaluated from proton inelastic scattering cross sections. When comparing these two measurement methods for  $0^+ \rightarrow 2^+$  transitions in nickel isotopes with  $N = 28-46$ , the values coming from purely electromagnetic probes appear lower than the inelastic proton scattering ones. This phenomenon is analogous to what was reported in ref. [10] for proton-closed-shell isotopes, and possibly linked to the additional contribution of the valence neutrons. Reference [8] reports on a recent  $(p, p')$  measurement for  $^{72,74}\text{Ni}$ . We report on the new studies of  $^{68,70}\text{Ni}(p, p')$  cross sections (or the proton inelastic scattering experiments on  $^{68-72}\text{Ni}$ ) that will complete the overall picture.

## 2. – Experimental details

The goal of this work is the measurement, in inverse kinematics, of the inelastic scattering cross section of  $^{68,70,72}\text{Ni}$  where the nuclei are left in the first  $2^+$  excited state. The experiment was carried out at the National Superconducting Cyclotron Laboratory (NSCL) of the Michigan State University (MSU). The building blocks of the setup are: production, identification and counting of the radioactive ions of interest; a thick hydrogen target; the measurement and identification of the reaction products and the rate of population of the  $2^+$  state. This is achieved by measuring the number of de-excitation gamma rays. Each step is briefly summarized in the following.

A primary beam of  $^{76}\text{Ge}^{30+}$  at 130 MeV/A hits a primary beryllium target where fragmentation reactions produce a wide range of ions that are then separated and selected using the A1900 fragment separator [11]. The A1900 eventually delivers a cocktail beam

where the nucleus of interest is mixed with a variety of contaminants. Three different settings of this spectrometer are used, one for each of the isotopes studied.

The S800 magnetic spectrometer is used [12]. It is composed of two main parts: the analysis line and the spectrograph. The first part of the setup allows the incoming beam identification and comprises a plastic scintillator and a silicon PIN detector (used only for the  $^{72}\text{Ni}$  setting), both are placed in-beam at the object position (OBJ). At the intermediate image station, two pairs of Parallel Plate Avalanche Counters (PPACs) allow the reconstruction of the position and the angle of the ions before the target. The S800 spectrograph, placed after the secondary target, is composed of a pair of dipole magnets followed by the focal plane (FP) station. This is instrumented with a pair of Cathode Readout Drift Chambers (CRDCs), a set of ionization chambers (ICs) and the E1 scintillator. This set of detectors allows for particle identification, momentum reconstruction after the target and triggering of the setup.

The liquid hydrogen target (Ursinus College Liquid Hydrogen Target facility of NSCL) is placed at the image point of the S800 analysis line. The thickness measured at the end of the experiment was found to be  $57.4\text{ mg/cm}^2$ . The Gamma-Ray Energy Tracking In-beam Nuclear Array (GRETINA), is a segmented gamma ray germanium detector [13]. The analysis of the pulse shapes at each of the segment's signals allows a precise reconstruction of the position of an energy deposit inside of the detector. This, in turn, allows tracking the energy loss of a photon, thus reducing the continuum in the gamma spectra by reconstructing the multiple interactions of the incoming gamma ray, and a better angular resolution hence improving the Doppler correction of the emitted gamma ray. This is important for the present work, where the gamma-ray emitting ions'  $\beta$  is of the order of 0.4.

### 3. – Data analysis

The data analysis can be subdivided in a series of stages. First the S800 spectrometer's detectors have to be equalized, then corrections have to be applied to the measured quantities used for the Particle IDentification (PID) in order to improve purity and rejection rates in the ion's selections. At this point, cuts on the species of interest and Doppler correction are carried out and the gamma-ray spectra can be evaluated. The gamma-ray yield is then extracted with the aid of a simulation. In this preliminary work the S800 equalization and the particle identification procedure are described.

*IC and CRDC equalization.* – Both the IC and CRDC ( $x$  positions) detectors are segmented. An equalization of their response is carried out by selecting one type of ion in the incoming beam using Time Of Flight information and looking at the reaction products on the focal plane. In this kind of experiment, after the target, particles with the same  $Z$  will have similar energy loss in all the chambers. Three outgoing species are selected and the response is aligned to the first chamber. In the case of CRDC, though, an iterative procedure is needed because the information on the hit channel depends on the charge center position, that is, in turn, dependent on the equalization.

*CRDC position calibration.* – The momentum reconstruction of the particles after the target is obtained using the inverse map of the S800 spectrograph. The absolute position information at the focal plane is needed in order to correctly perform the inverse mapping. Such calibration is obtained using a mask with holes at known and fixed positions that is placed in front of the CRDCs. This allows to evaluate the

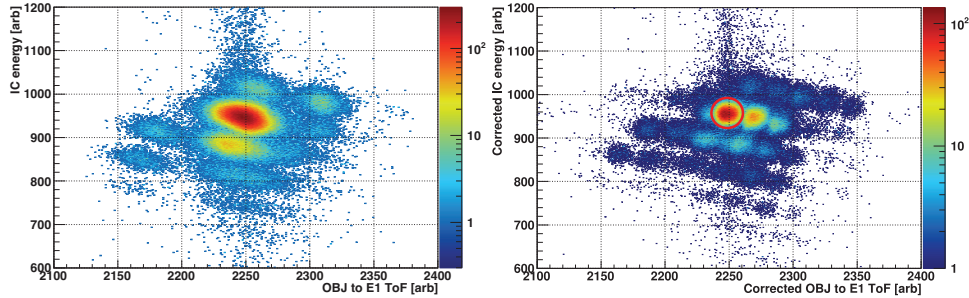


Fig. 1. – PID histograms for the  $^{70}\text{Ni}$  setting. Only S800 events in coincidence with GRETINA are displayed. The left and right pictures show respectively uncorrected and corrected variables. The circled peak in the right picture corresponds to  $^{70}\text{Ni}$ , with decreasing  $A$  from left to right, while  $Z$  increases from bottom to top.

offset in the  $x$ -direction and to calibrate the drift time into  $y$ -axis absolute focal plane positions.

*PID corrections.* – To identify each particle’s  $A$  and  $Z$  after the target, a 2D histogram of the energy deposited in the IC with respect to the ToF from the OBJ station to the E1 focal plane scintillator is performed. The result is shown in the left panel of fig. 1. Both these observables, though, depend on the particle’s trajectory inside the spectrometer. In order to improve the identification capabilities of the setup, a correction as a function of the particle position at the focal plane and its angle in the dispersive direction is carried out. The result of this procedure is shown in the right panel of fig. 1. The separation of various mass numbers along the horizontal lines is clearly visible.

#### 4. – Conclusions and perspectives

The importance of investigating the nuclear shell evolution with both hadronic and purely electromagnetic probes has been discussed for the nickel isotopic chain. The preliminary analysis of an inelastic proton scattering experiment on  $^{68-72}\text{Ni}$  has been reported. In particular, the calibration of the S800 detectors and PID optimization was reviewed. This work will serve as the starting point for the following gamma-ray spectra analysis and the cross sections measurement.

#### REFERENCES

- [1] OTSUKA T. *et al.*, *Rev. Mod. Phys.*, **92** (2020) 015002.
- [2] ALDER K. *et al.*, *Rev. Mod. Phys.*, **28** (1956) 432.
- [3] PRITYCHENKO B. *et al.*, *At. Data Nucl. Data Tables*, **98** (2012) 798.
- [4] PERRU O. *et al.*, *Phys. Rev. Lett.*, **96** (2006) 232501.
- [5] AOI N. *et al.*, *Phys. Rev. Lett. B*, **692** (2010) 302.
- [6] MARCHI T. *et al.*, *Phys. Rev. Lett.*, **18** (2014) 182501.
- [7] KOLOS K. *et al.*, *Phys. Rev. Lett.*, **116** (2016) 122502.
- [8] CORTÉS M. L. *et al.*, *Phys. Rev. C*, **97** (2018) 044315.
- [9] GOTTARDO A. *et al.*, *Phys. Rev. C*, **102** (2020) 014323.
- [10] BERNSTEIN A. M. *et al.*, *Phys. Lett. B*, **103** (1981) 255.
- [11] MORRISSEY D. J. *et al.*, *Nucl. Instrum. Methods Phys. Res., Sect. B*, **204** (2003) 90.
- [12] BAZIN D. *et al.*, *Nucl. Instrum. Methods Phys. Res., Sect. B*, **204** (2003) 629.
- [13] PASCHALIS S. *et al.*, *Nucl. Instrum. Methods Phys. Res., Sect. A*, **709** (2013) 44.